

## Chapter 4 FaBCoM TeSt Experimental Modal Analysis

### 4.1. Purpose

The main purpose of the EMA is to test the validity of the FEM developed in Patran.

### 4.2. Description

The analysis was performed for a stationary structure with no damage. Measurements were taken at twelve points per blade as well as at the point of excitation (Ref 1) as shown in Figure 4-1:

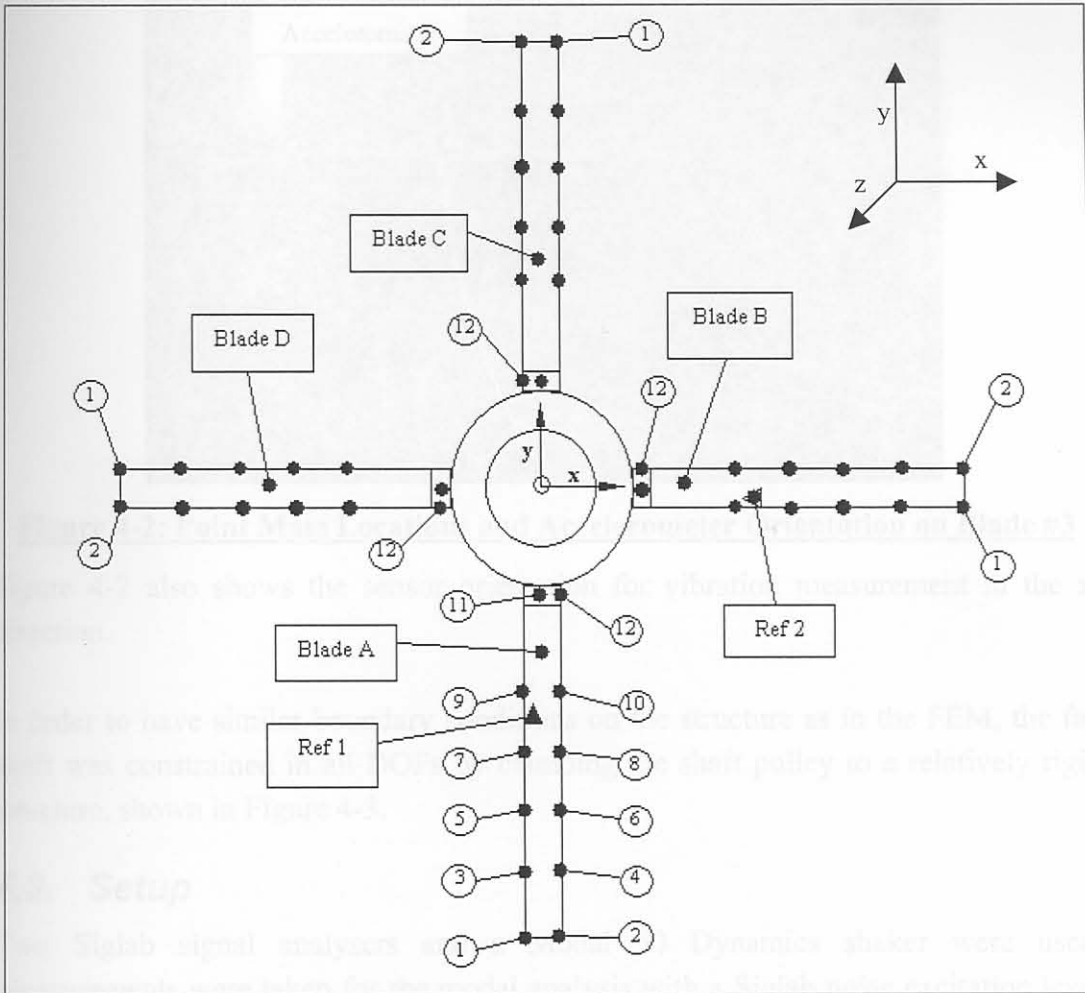


**Figure 4-1: FaBCoM TeSt EMA Measurement Point Positions**

Four PCB piezoelectric accelerometers were used (one for each blade) as well as an impedance head (consisting of a force transducer as well as an accelerometer) at the excitation points for transducers. The point Ref 2 was only used during the reciprocity test. Measurements were taken in the z-direction at all points except the 12<sup>th</sup> point on each blade. Also, sideways vibration measurements were taken at points 1, 3, 7, 9 and 12 of each blade. The positions of the sensors were obtained from the positions of nodes of maximum displacement at the 42<sup>nd</sup> mode shape obtained from the FEM, as this mode shape is the most complex mode shape in terms of flap wise

blade vibration within a 2000 Hz bandwidth. The position of the sensors can be found in table A-1 in Appendix A. The  $10^\circ$  blade angle was not taken into account.

As it was discovered in the sensitivity analysis that added point masses do have influences on some modal frequencies, it was decided to add point masses at points 1 to 10 on each blade with the same mass as that of the accelerometer used on each particular blade as shown in Figure 4-2:

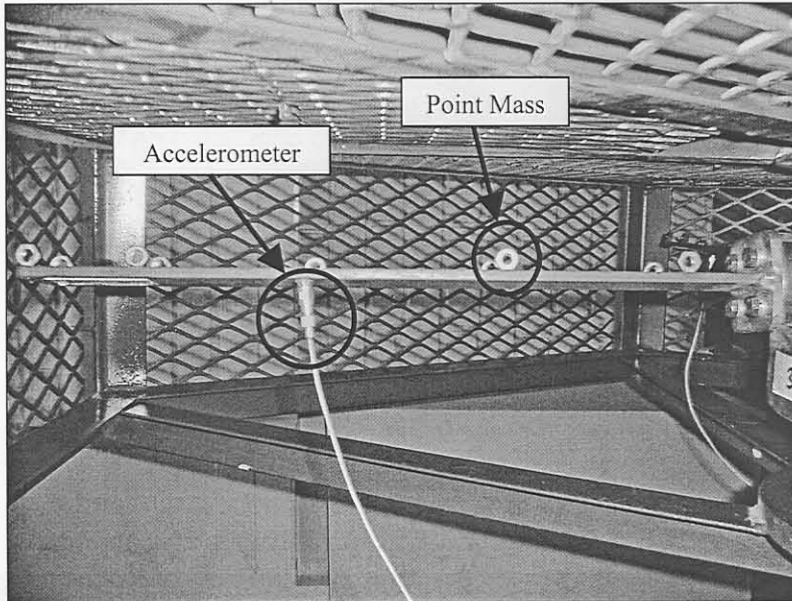


**Figure 4-2: Point Mass Locations and Accelerometer Orientation on Blade #3**

Figure 4-2 also shows the sensor orientation for vibration measurement in the z-direction.

In order to have similar boundary conditions on the structure as in the FEM, the fan shaft was constrained in all DOFs by clamping the shaft pulley to a relatively rigid structure, shown in Figure 4-3.

### 4.3. Setup

Two Siglab signal analysers and a Modal 50 Dynamics shaker were used. Measurements were taken for the modal analysis with a Siglab noise excitation level of 0.5 V RMS and an amplifier output level of 50%. Figure 4-4 shows the orientation of the Modal 50 Dynamics shaker with regards to the test structure. Figure 4-5 shows the excitation point on blade #1 with the impedance head in position as well as a sideways-orientated accelerometer. Figure 4-6 shows the overall telemetry setup with the two Siglabs and some PCB signal conditioning equipment for the accelerometers.



**Figure 4-3: Shaft Clamping**

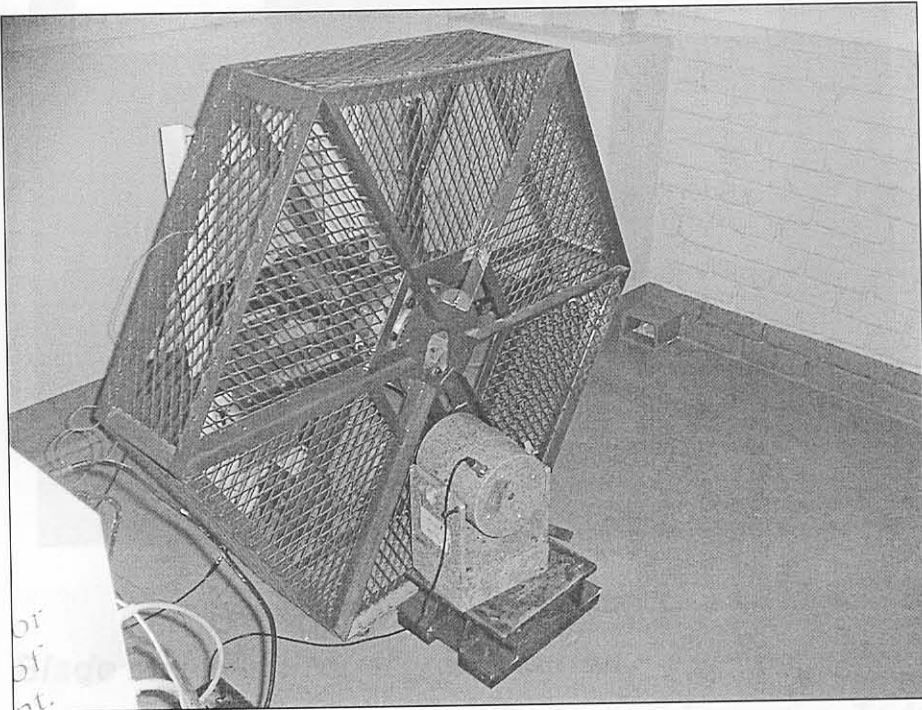


**Figure 4-4: Modal 50 Shaker Orientation**

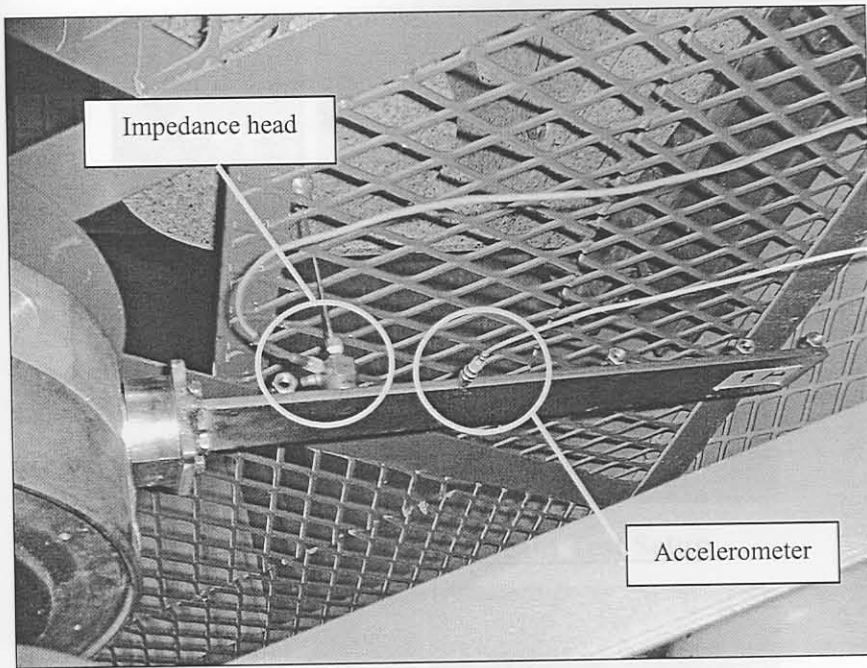


**Figure 4-5: Excitation Point and Sideways-Orientated Accelerometer**

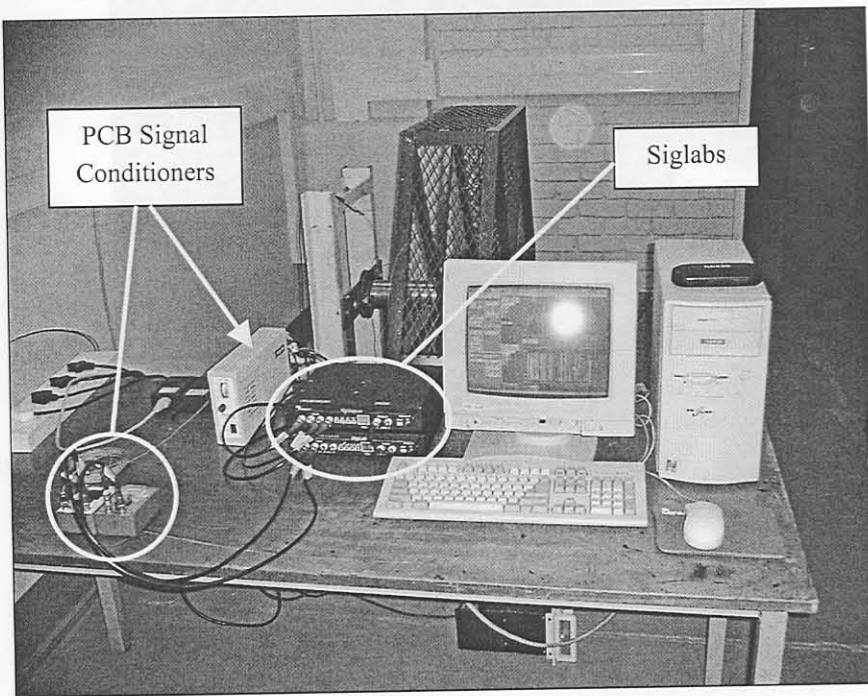


**Figure 4-6: Telemetry Setup**

#### **4.4. Blade Material Property Extraction**

The FEM results were found to be very sensitive to material properties. To determine the material properties of the steel used to manufacture the fan blades, the 1<sup>st</sup> natural frequency of a free-free beam of the same batch of steel was measured over a bandwidth of 500 Hz with excitation provided by a modal hammer. The test setup is shown in Figure 4-7 and Figure 4-8:

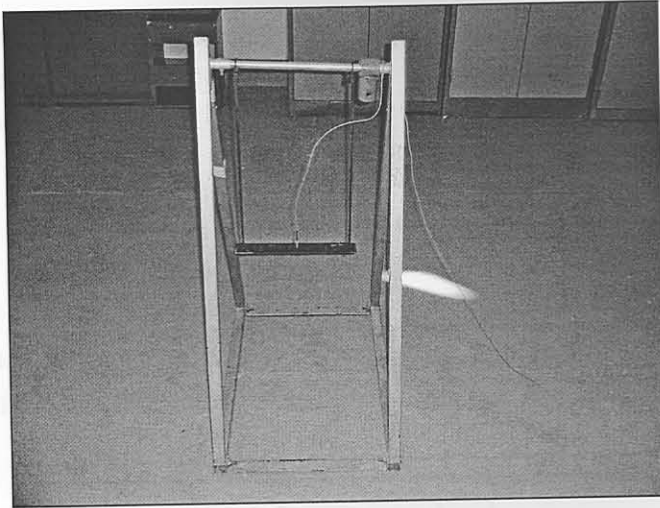


**Figure 4-7: Free-free Beam Test Setup**

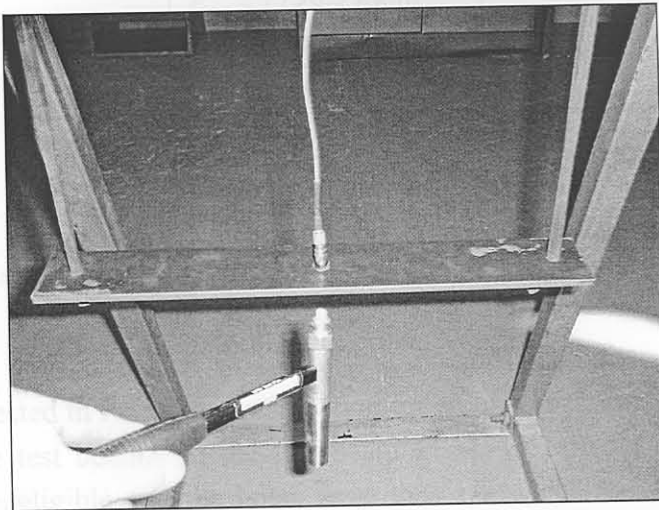


**Figure 4-8: Beam Test**

The measured FFT of the beam is shown in Figure 4-9:

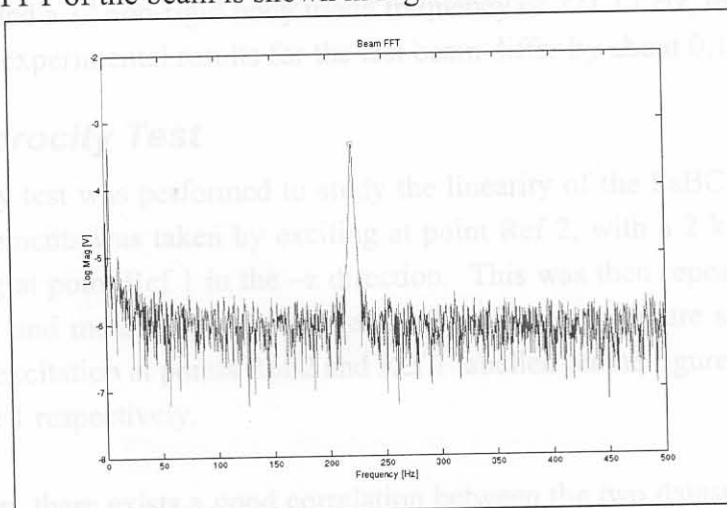


**Figure 4-9: Beam FFT over 500 Hz Bandwidth**

The 1<sup>st</sup> natural frequency of the test beam was found to be at 221.56 Hz. The material properties of a beam can be calculated from its 1<sup>st</sup> natural frequency using Equation (4-1) obtained from Rao [41]:

$$\omega = (\beta l)^2 \sqrt{\frac{E_y I}{\rho A l^4}} \quad (4-1)$$

Table 4-1 lists the values of the variables used with  $\omega$  obtained from Figure 4-9 and  $\rho$ ,  $A$ ,  $l$  and  $I$  measured from the test specimen.  $\beta l = \pi$  is given by Rao [41].

**Table 4-1: Variable Values for Equation ( 4-1 )**

$\omega$	1392.1 rad.s <sup>-1</sup>
$\rho$	7756.3 kg.m <sup>-3</sup>
$A$	2.5x10 <sup>-4</sup> m <sup>2</sup>
$l$	0.34 m
$I$	5.208x10 <sup>-10</sup> m <sup>4</sup>
$\beta l$	$\pi$

From Equation ( 4-1 ), Young's modulus for the material is calculated as

$$E_y \approx 192.6 \text{ GPa}$$

This result was tested in Patran for verification for an unconstrained beam of the exact properties of the test beam. In the test beam FEM, the effects of the holes were assumed to be negligible and the holes were thus excluded from the FEM. Figure 4-10 shows the 1<sup>st</sup> mode shape deflection of the FEM.

The FEM yielded a 1<sup>st</sup> non-rigid body mode frequency of 221.17 Hz, meaning that the numerical and experimental results for the test beam differ by about 0.18%.

#### 4.5. Reciprocity Test

The reciprocity test was performed to study the linearity of the FaBCoM TeSt. One set of measurements was taken by exciting at point Ref 2, with a 2 kHz sine sweep, and measuring at point Ref 1 in the  $-z$  direction. This was then repeated by exciting at point Ref 1 and measuring at point Ref 2. The following figure shows the FRFs measured for excitation at points Ref 2 and Ref 1 labelled on the figure as Reference 2 and Reference 1 respectively.

As can be seen, there exists a good correlation between the two datasets up to 1 kHz. Beyond that, the correlation is not as good, but still very much acceptable.

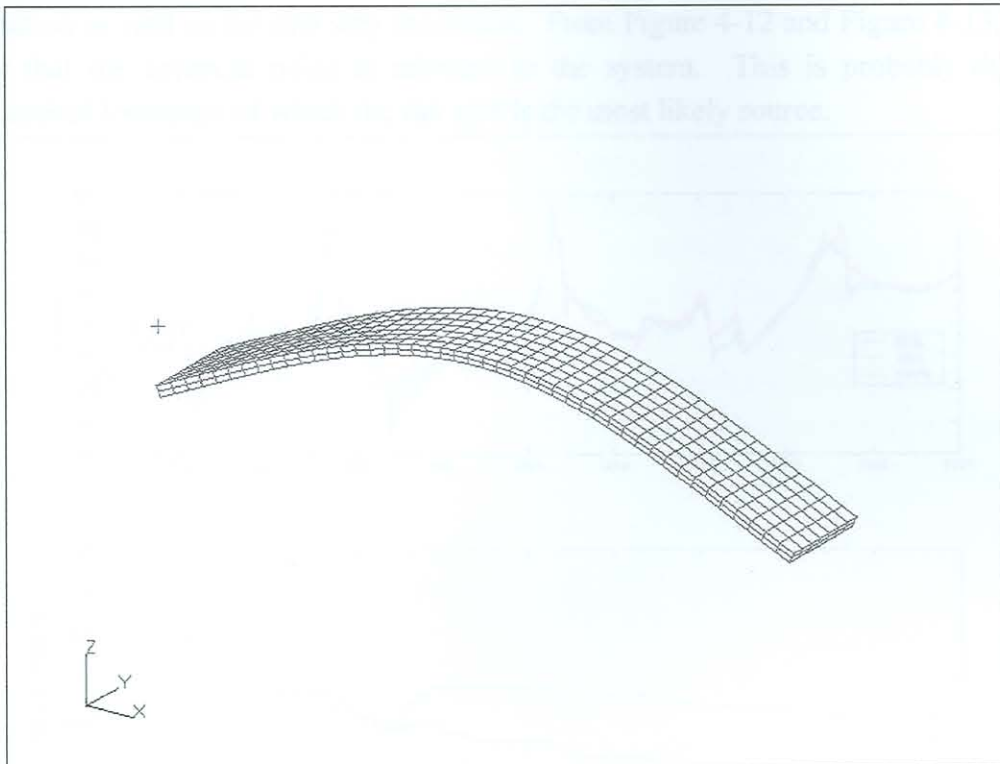


**Figure 4-10: Beam Test FEM**

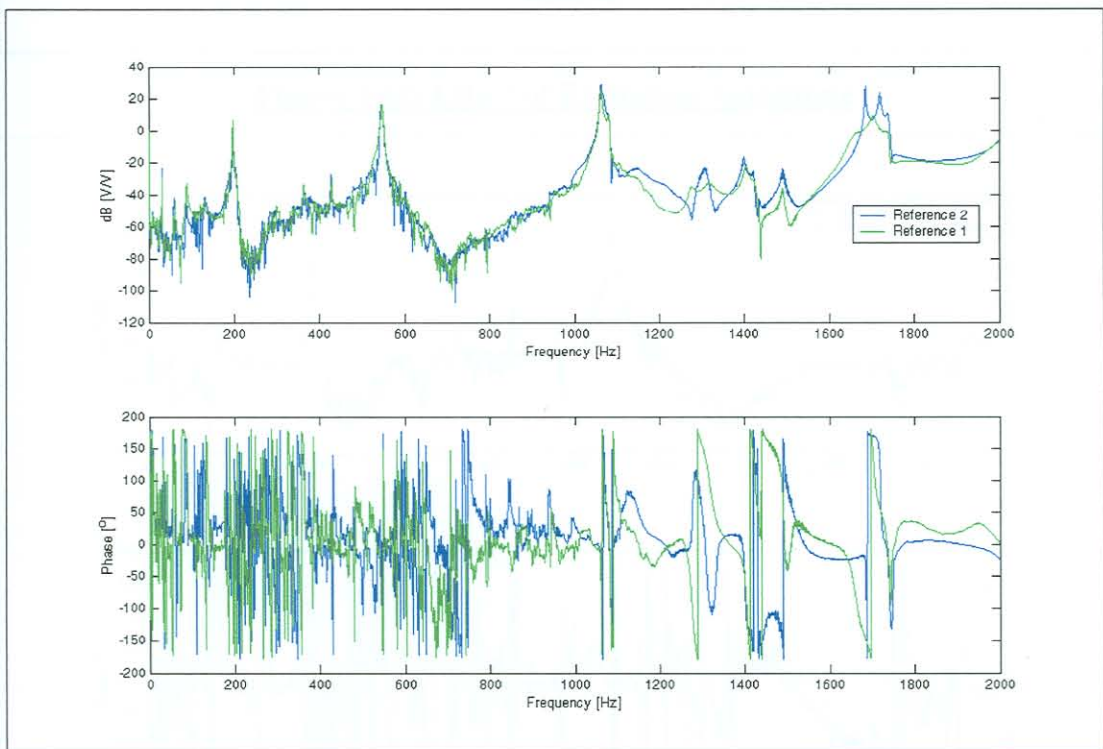


**Figure 4-11: Reciprocity Test Results**

#### 4.5.1. Noise Quantification and Qualification

From Figure 4-11, it seems that the FRFs are very noisy below 1 kHz. This was investigated by resampling the data for excitation at Ref 1 for different levels of

excitation as well as for sine step excitation. From Figure 4-12 and Figure 4-13, it is clear that the apparent noise is inherent to the system. This is probably due to mechanical looseness of which the fan grid is the most likely source.

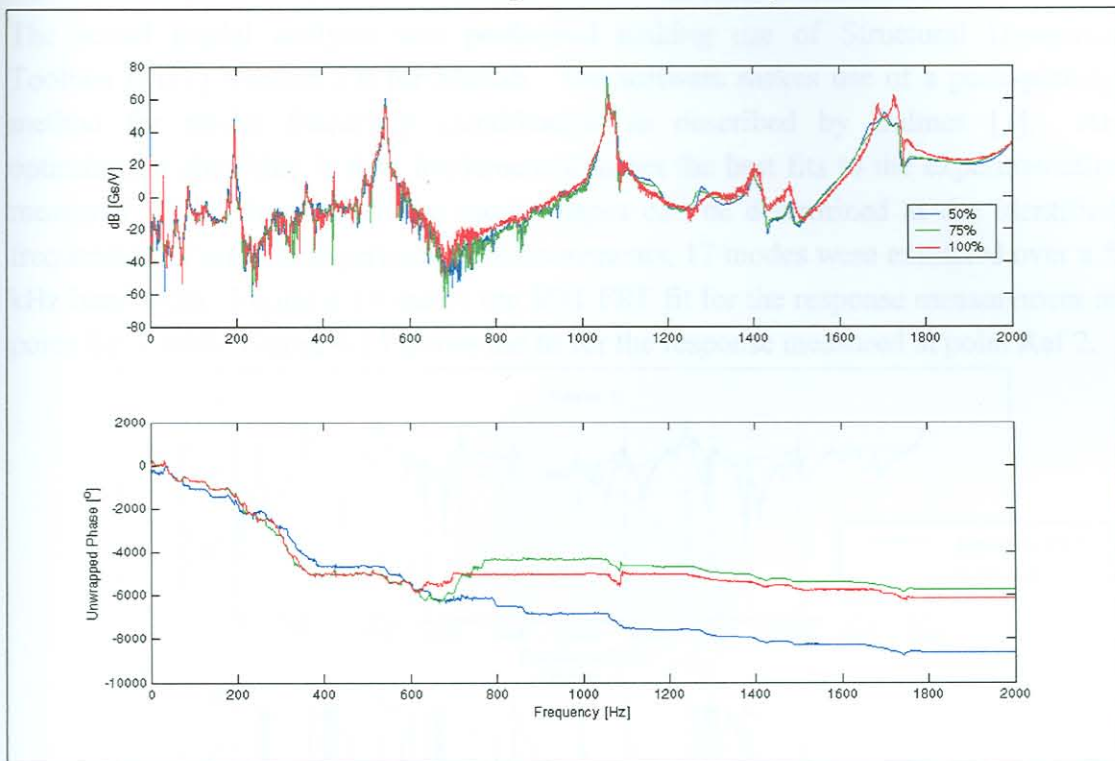


**Figure 4-12: Effect of Excitation Amplitude**

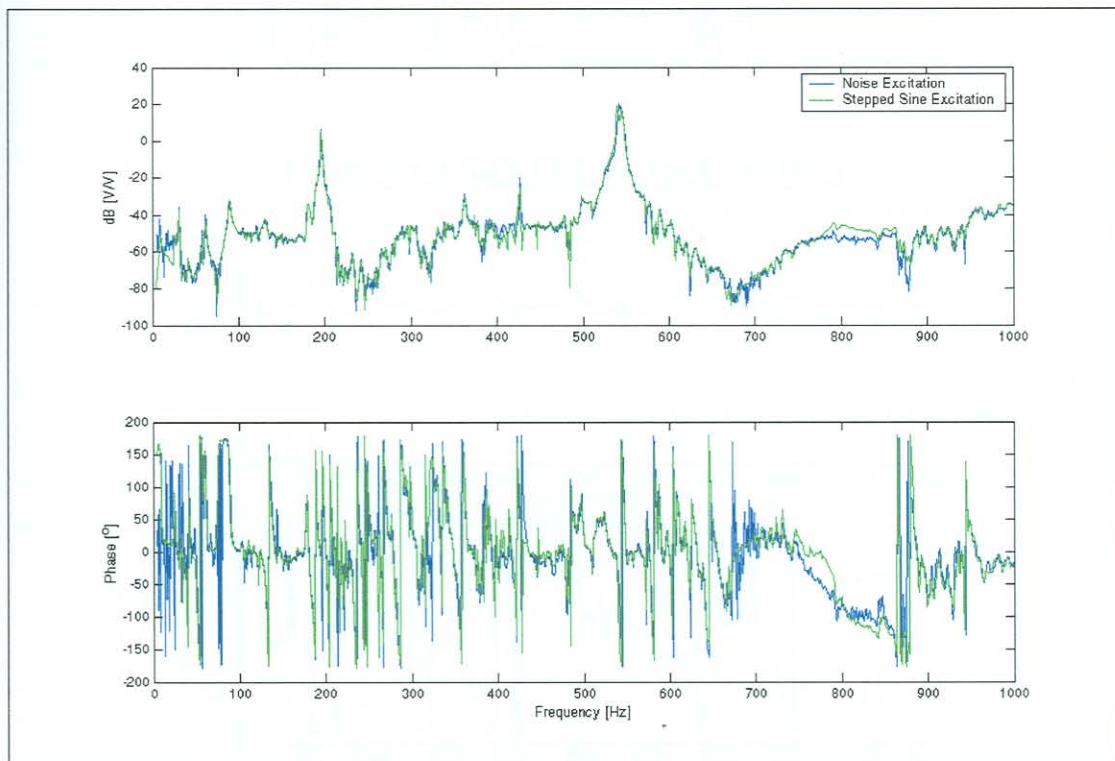


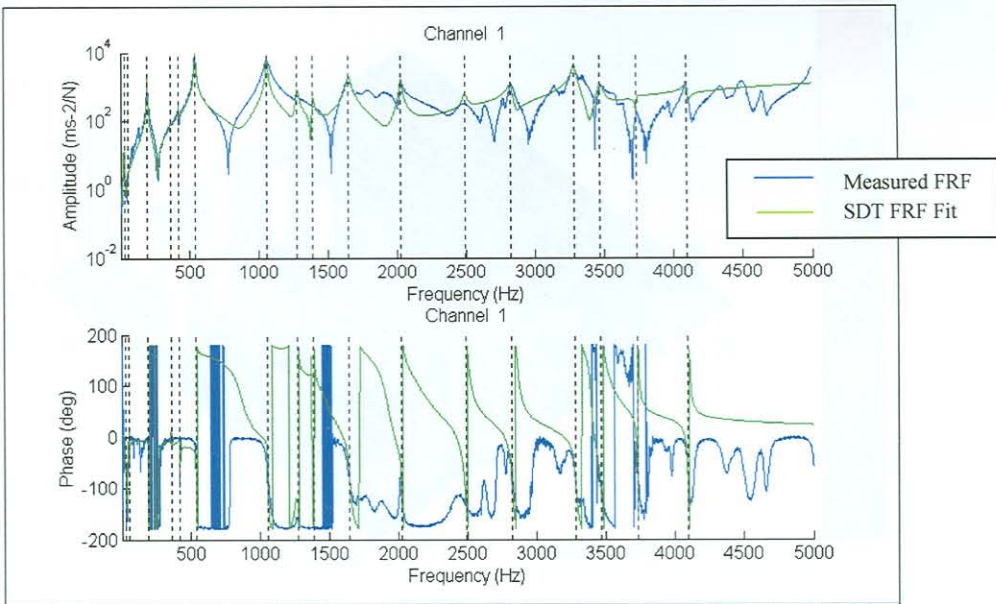
**Figure 4-13: Noise and Stepped Sine Excitation Comparison**



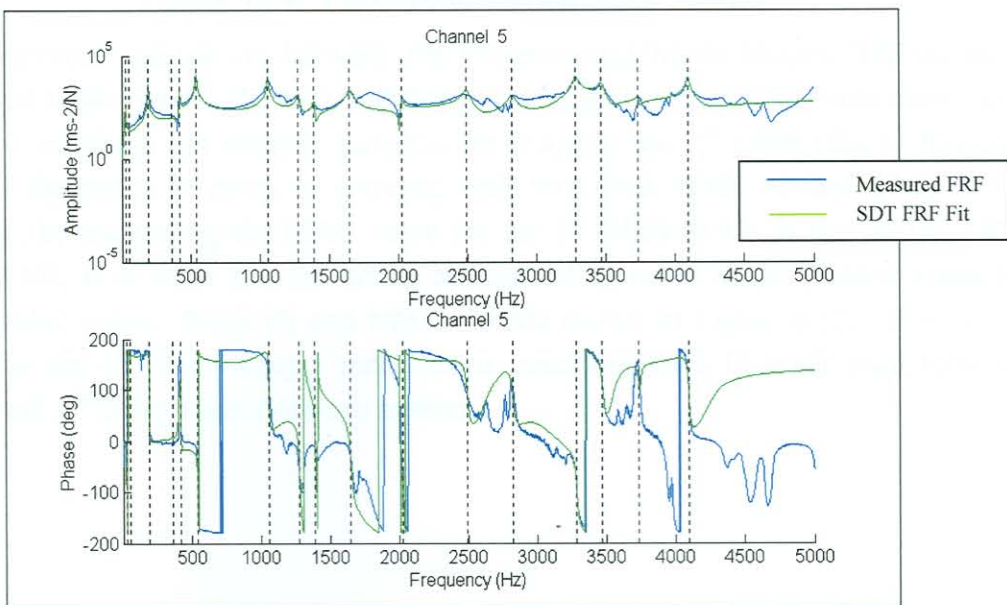
## 4.6. Modal Analysis

### 4.6.1. Modal Parameter Extraction

The actual modal analysis was performed making use of Structural Dynamics Toolbox (SDT) Version 3.0 for Matlab. The software makes use of a peak-picking method for modal frequency identification as described by Balmes [1]. An optimisation algorithm is then implemented to get the best fits to the experimentally measured FRFs, from which the mode shapes can be determined at the identified frequencies. From the experimental measurements, 17 modes were extracted over a 5 kHz bandwidth. Figure 4-14 shows the SDT FRF fit for the response measurement at point Ref 1 while Figure 4-15 shows the fit for the response measured at point Ref 2.



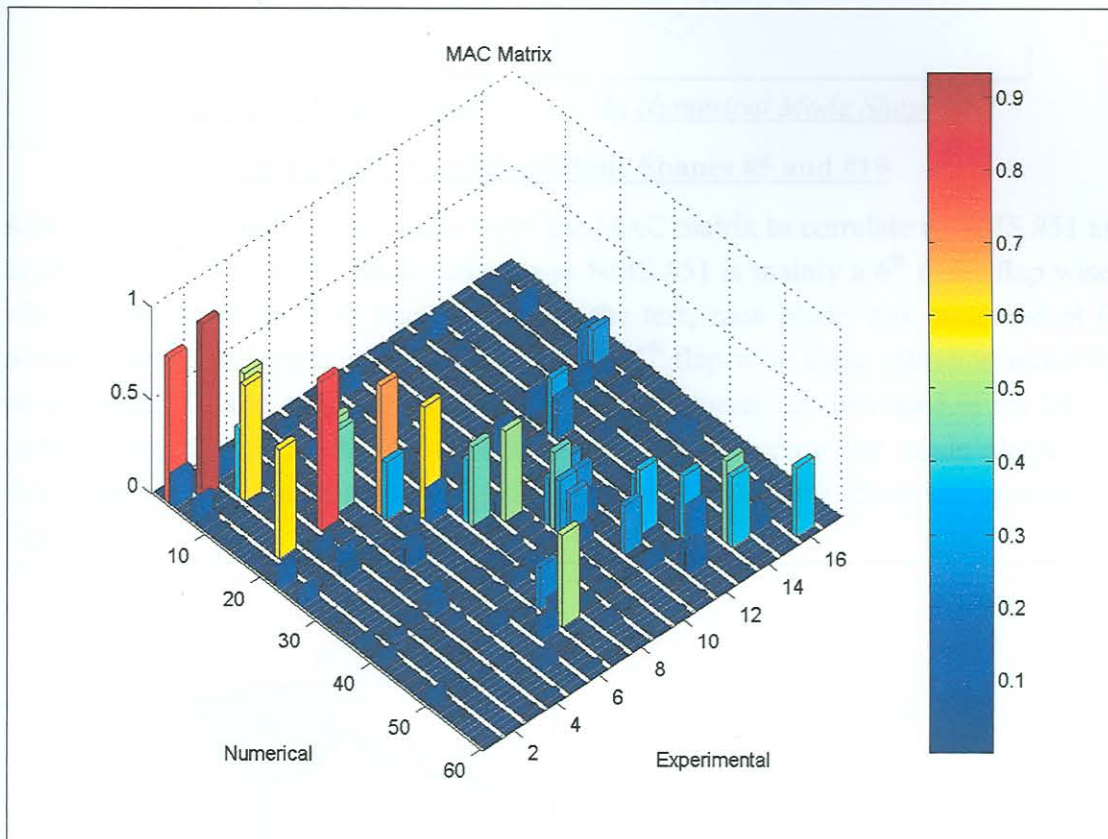
**Figure 4-14: SDT FRF Fit for Point Ref 1**



**Figure 4-15: SDT FRF Fit for Point 2 on Blade #1, Sideways**

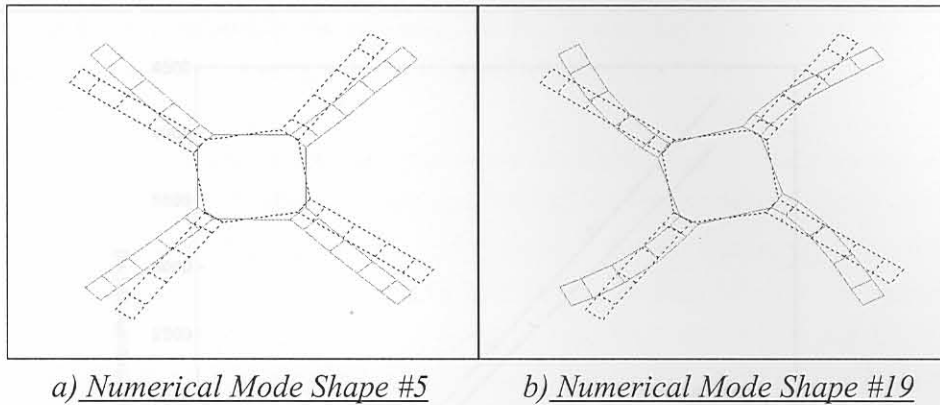
#### 4.6.2. MAC Matrix Calculations

Figure 4-16 shows the results for the MAC matrix in a three dimensional format. A definite diagonal can be seen on the MAC matrices. Few of the values however, are very good. Possible reasons include that only one shaker was used in the test that may have resulted in insufficient amounts of energy supplied throughout the system for well defined responses.



**Figure 4-16: Three Dimensional MAC Matrix**

From graphical comparison between the Experimental Mode Shapes (EMSs) and Numerical Mode Shapes (NMSs) with MAC values greater than 0.3, it was clear that the MAC matrix is not entirely accurate, for example the 2<sup>nd</sup> EMS (the 1<sup>st</sup> torsion mode of the shaft) is given to correlate well with both NMS #5 and NMS #19. However, by comparing the MAC value for the 5<sup>th</sup> NMS (0.93) to that of the 19<sup>th</sup> NMS (0.58), it is clear that the actual corresponding mode shape yielded a much higher MAC value. NMS #5 and NMS #19 are shown in Figure 4-17. The same occurs for the 4<sup>th</sup> EMS being a mode shape consisting of a 1<sup>st</sup> order shaft torsion motion and 2<sup>nd</sup> order blade sideways motion.



**Figure 4-17: Numerical Mode Shapes #5 and #19**

Also, EMS #7, at 1058.9 Hz, is shown by the MAC matrix to correlate to NMS #51 at 2630.6 Hz. This is due to modal aliasing as NMS #51 is mainly a 6<sup>th</sup> order flap wise vibration mode of the four blades. During the test, each blade was measured at 6 positions along its length, allowing for only the 5<sup>th</sup> flap-wise blade vibration mode to be detected. This in effect is the same case for the numerical data used in the MAC matrix computation, as the software used can only compare the mode shapes of structures with an equal number of nodes. The modal aliasing effect can be seen in Figure 4-18.

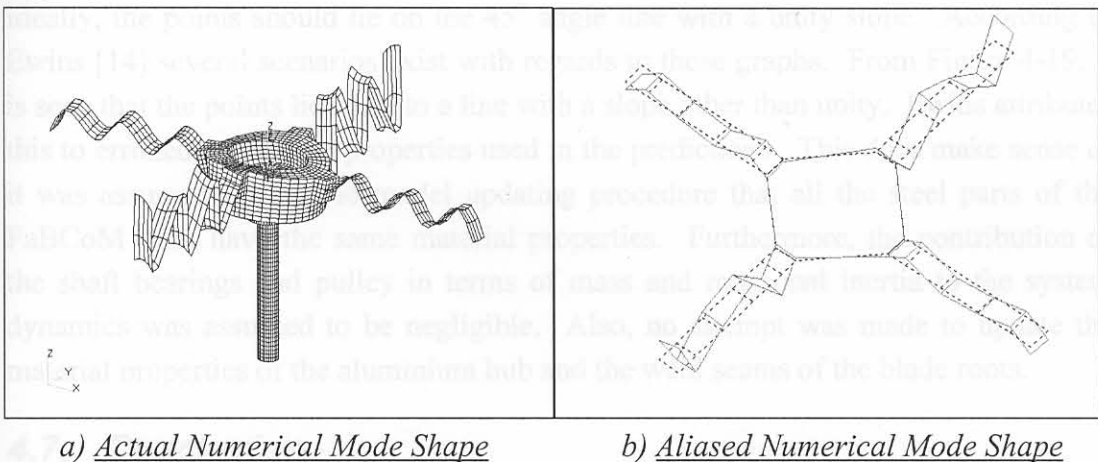


**Figure 4-18: Modal Aliasing of Numerical Mode Shape #51**

When these discrepant mode shapes are ignored when a scatter plot of the numerical and experimental frequencies is drawn, Figure 4-19 is obtained. Equation ( 4-2 ) gives the function of the linear fit calculated using Excel and Matlab:

$$f_{\text{exp}} = 1.1034f_{\text{num}} - 55.166 \quad (4-2)$$

with  $R^2 = 0.9902$ .

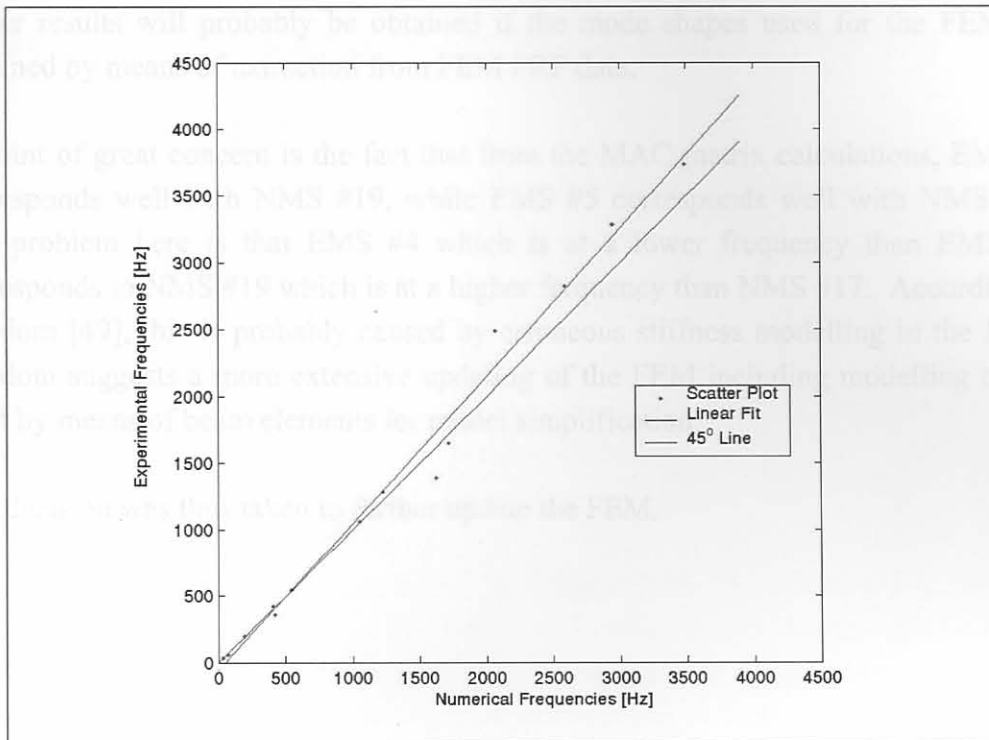


**Figure 4-19: Comparison of Experimental and Numerical Natural Frequencies**

Ideally, the points should lie on the  $45^\circ$  angle line with a unity slope. According to Ewins [14] several scenarios exist with regards to these graphs. From Figure 4-19, it is seen that the points lie close to a line with a slope other than unity. Ewins attributes this to erroneous material properties used in the predictions. This does make sense as it was assumed during the model updating procedure that all the steel parts of the FaBCoM TeSt have the same material properties. Furthermore, the contribution of the shaft bearings and pulley in terms of mass and rotational inertia to the system dynamics was assumed to be negligible. Also, no attempt was made to update the material properties of the aluminium hub and the weld seams of the blade roots.

#### 4.7. Conclusion

Although not extremely good values were obtained from the MAC matrix, a well-defined diagonal does exist. This means that the FEM does correspond sufficiently to the FaBCoM TeSt in terms of mode shapes. One reason for the poor overall MAC values may be the assumptions used in the FEM as described in Section 2.7. To obtain better results, a more intensive model updating procedure of the FEM is necessary.

Another likely reason for the low MAC values is the effect of modal density as up to four mode shapes of the FEM were found at around the same frequency as described in Section 3.5. During calculation of the MAC matrix, each EMS is compared to each NMS. This presents a problem, as closely spaced mode shapes around some frequency will appear as a single hybrid mode shape in the experimental structure.

Better results will probably be obtained if the mode shapes used for the FEM are obtained by means of extraction from FEM FRF data.

A point of great concern is the fact that from the MAC matrix calculations, EMS #4 corresponds well with NMS #19, while EMS #5 corresponds well with NMS #17. The problem here is that EMS #4 which is at a lower frequency than EMS #5, corresponds to NMS #19 which is at a higher frequency than NMS #17. According to Strydom [49], this is probably caused by erroneous stiffness modelling in the FEM. Strydom suggests a more extensive updating of the FEM including modelling of the shaft by means of beam elements for model simplification.

The decision was thus taken to further update the FEM.

The first torsional modal frequency of the FEM (NMS #5) was tuned to the first torsional NMS frequency (EMS #2). This was decided upon in the aim of correlating the frequencies of NMS #19 to EMS #4 (the second shell-rotated torsional mode shape) as these mode shapes prove to be very important in terms of damage detection as illustrated by Mawardi and Threshaway [35] and noted in Section 3.4.

In order to do this, it was decided to revise the design of the FEM. The solid element modelled shaft was replaced with a beam element modelled shaft. The reason for this is that it is much easier to adjust the diameter of the modelled shaft when beam elements are used as opposed to solid elements. This also serves to simplify the model (4-9). The beam element modelled shaft was connected to the rest of the FEM by means of an RBE2-type MPC as shown in Figure 5-1. The same nodal constraints were applied here as on the shaft of the previous FEM.

By performing modal analyses on the FEM for arbitrarily chosen shaft radii, a graph was drawn up relating the frequencies of NMS #5 to the different shaft radii as shown in Figure 5-2. A shaft radius that will yield the desired frequency was calculated as 21.08 mm. By updating the FEM accordingly, NMS #5 was changed from 68.3 Hz in the initial FEM to 57.28 Hz, corresponding very well with the 57.24 Hz frequency of EMS #2.

The frequency of the NMS corresponding with EMS #4 shifted from 416.96 Hz to 393.97 Hz, moving closer to the frequency of EMS #4 which is 361.07 Hz. This improved the frequency error from 15.5% to 6.4%.